

Room Temperature On-Off Operation of Current in He Ion Irradiated Graphene Sheet

Shu Nakaharai¹, Tomohiko Iijima², Shinichi Ogawa³, Shingo Suzuki¹, Hisao Miyazaki⁴, Songlin Li⁴, Kazuhito Tsukagoshi⁴, Shintaro Sato¹ and Naoki Yokoyama¹

¹Green Nanoelectronics Center, ²Innovation Center for Advanced Nanodevices, ³Nanoelectronics Research Institute, AIST, 16-1 Onogawa, Tsukuba, Ibaraki 305-8569, Japan

Phone: +81-29-849-1483, E-mail: shu-nakaharai@aist.go.jp

⁴WPI-MANA, NIMS,

1-1 Namiki, Tsukuba, Ibaraki 305-0044, Japan

1. Introduction

Graphene, a two-dimensional sheet of carbon atoms [1], has been expected for channel material of transistors in super high-speed and ultra-low power consumption LSIs. The absence of bandgap, however, is still one of the most serious bottlenecks for logic application. Graphene nanoribbon (GNR) is one of the solutions for this issue [2], but it requires an extremely high precision in ribbon width because electrical properties such as a bandgap value depend on the ribbon width, which may cause severe variations in electrical properties. For industrial feasibility, therefore, graphene should be used in a *bulk* form rather than a tiny structure. For this reason, bandgap engineering by chemical functionalization has been actively investigated, including graphene oxide [3], hydrogenated graphene (graphane) [4], chlorinated graphene [5] and fluorinated graphene [6]. Although some of these techniques succeeded in bandgap opening, they still have difficulties in controlling the density of functionalizing atoms on graphene and also experience the instability of the functionalizing atoms (migration or desorption) during heating or the lithography process. Another bandgap opening technique with *bulk* graphene is defect engineering [7-10], in which atomic vacancies, Stone-Wales (SW) defects [11] or other kinds of imperfection in the honeycomb structure of graphene lattice break the symmetry of electron states, resulting in bandgap opening. For example, it is argued theoretically that vacancies or SW defects can induce a bandgap up to 0.25 eV [10]. However, the on-off operation of current by gate bias has not yet been demonstrated experimentally in defected graphene which is irradiated by an ion or electron beam [12,13].

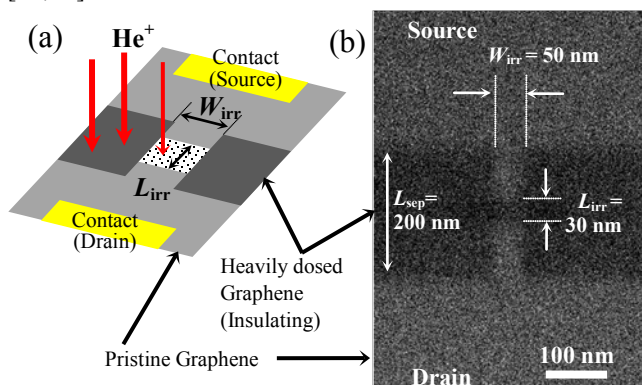


Fig. 1. (a) Schematic illustration of the fabricated device. Charge transport through the central part of $W_{\text{irr}} \times L_{\text{irr}}$ with a controlled He ion dose is examined in this work. (b) A helium ion microscope image of a fabricated device.

In this work, we present the functionalization of graphene by He ion irradiation, and demonstrate the first room temperature on-off operation of current up to two orders of magnitude by back gate bias sweeping in defect-engineered graphene. Characterization of the activation energy of thermally activated carrier transport in the irradiated graphene is also presented.

2. Experimental Results and Discussion

Single layer graphene flakes were mechanically exfoliated from a crystal of HOPG using adhesive tape, and then deposited on a silicon wafer with a 285-nm-thick surface thermal oxide layer. The number of graphene layers was identified with an optical microscope [14]. On the obtained graphene flakes, source and drain contacts were patterned by electron-beam lithography, and a Ti/Au (5/30 nm) layer was formed by thermal evaporation.

Helium ion beams were applied to the graphene flakes using He Ion Microscope (HIM) which can also be used for graphene etching [15,16]. The central region of the device (Fig. 1) with a width, W_{irr} , of 50 nm and a length, L_{irr} , of 30 nm was exposed to a He ion beam with controlled doses from 2.2×10^{15} to 1.3×10^{16} ions/cm². Except for this region, source and drain regions were separated by heavily dosed (1.3×10^{16} ions/cm²) regions with a length, L_{sep} , of 200 nm. It was confirmed that the current across this heavily dosed region was much lower than 1 pA at drain bias, V_{D} , up to 10 V, indicating that the current flowing through the device is dominated by the resistance in the central region of $L_{\text{irr}} \times W_{\text{irr}}$. Two-terminal DC drain current, I_{D} , was measured with sweeping V_{D} or back gate bias, V_{BG} , at various temperatures from 20 K to 300 K.

Figure 2(a) shows the ion dose dependence of I_{D} at room temperature. Here, I_{D} is plotted for different V_{D} 's. As shown in the figure, I_{D} decays exponentially as the ion dose

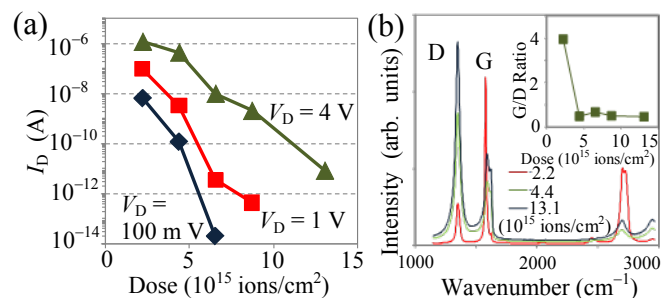


Fig. 2. (a) Helium ion dose dependence of I_{D} at different V_{D} , at room temperature. (b) Raman spectra of He ion irradiated graphene with different ion doses. The ion dose dependence of G/D ratio is also shown in the inset.

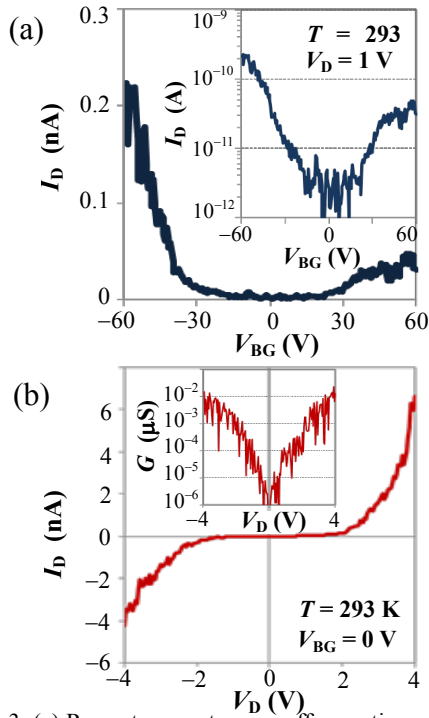


Fig. 3. (a) Room temperature on-off operation of drain current in graphene with an ion dose of 8.7×10^{15} ions/cm². The log-scale plot in the inset shows on-off ratio of two-order of magnitude. (b) Drain bias dependence of drain current at room temperature, and its differential conductance in the inset.

increases. The crystal quality of irradiated graphene was observed by Raman spectroscopy, and some of the spectra and G/D ratio are shown in Fig. 2(b). Even at the highest dose in Fig. 2, G mode peak is still apparent, suggesting that the honeycomb structure of graphene remains in spite of the induced defects and the low values of I_D .

On-off operation of I_D by sweeping V_{BG} at room temperature in a sample with an ion dose of 8.7×10^{15} ions/cm² is shown Fig. 3(a). As shown in the logarithmic plot in the inset, the on-off ratio is about two orders of magnitude. Figure 3(b) shows the I_D - V_D characteristics of the same sample, along with the differential conductance $G = |dI_D/dV_D|$ shown in the inset. The plateau of I_D - V_D curve and hence the conductance drop at $V_D = 0$ V also suggest strong suppression of carrier transport around the charge neutrality point in the He ion irradiated graphene.

Temperature dependence of conductance minimum, G_{\min} , allows us to estimate the bandgap value as the activation energy, E_A , of thermally activated transport scheme,

$$G_{\min} \propto \exp\left(\frac{-E_A}{2k_B T}\right), \quad (1)$$

where k_B is the Boltzmann's constant. Figure 4(a) shows the G - V_D characteristics at different temperatures of 300, 100 and 20 K in the sample with an ion dose of 6.5×10^{15} ions/cm². As shown in Fig. 4(a), the conductance shows a minimum, G_{\min} , at $V_D = 0$ V, and G_{\min} decays rapidly as the temperature decreases. Temperature dependence of G_{\min} of samples with ion doses of 4.4×10^{15} and 6.5×10^{15} ions/cm² is plotted in Fig. 4(b). From these plots, E_A for each sample has been derived from formula (1), obtaining 38 meV and 260 meV for samples with the ion doses of 4.4×10^{15} and

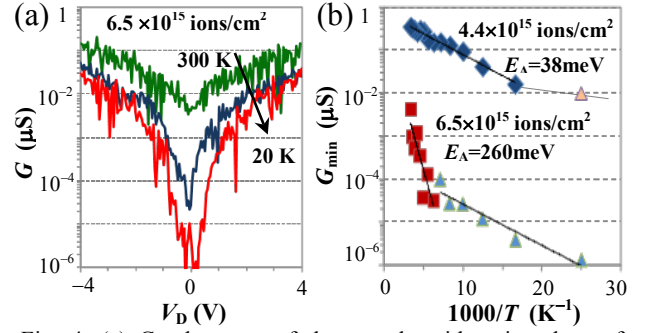


Fig. 4. (a) Conductance of the sample with anion dose of 6.5×10^{15} ions/cm² at $T = 300, 100$ and 20 K. (b) Temperature dependence of the conductance minimum at $V_D = 0$ V of the samples with ion doses of 4.4×10^{15} ions/cm² and 6.5×10^{15} ions/cm², and their activation energy is evaluated.

6.5×10^{15} ions/cm², respectively. Here, in both samples, thermally activated transport scheme appears in higher temperatures, while G_{\min} deviates from the Arrhenius fitting line in low temperatures. These behaviors of temperature dependence are quite similar to those in GNRs [17], in which E_A and other electrical properties depend on the ribbon width, while E_A depends strongly on the ion dose in our case of irradiated graphene.

Finally, in spite of the excellent controllability of carrier transport properties by He ion doses, it is also found that the electrical properties are easily affected by contaminations on the surface. Consequently, surface treatment should be critical for further improvement in of the graphene functionalization by ion irradiation.

3. Summary

In summary, we have realized the functionalization of graphene by He ion irradiation, and demonstrated the room temperature on-off operation of drain current by back gate bias sweeping with an on-off ratio of about two orders of magnitude. From the temperature dependence of G_{\min} , we evaluated the activation energy of thermally activated transport, which was found to be strongly sensitive to the He ion dose.

Acknowledgements

This research is granted by JSPS through FIRST Program initiated by CSTP.

References

- [1] K. Novoselov, *et al.*, Science **306**, 666 (2004).
- [2] S. Nakaharai, *et al.*, *Ext. Abst. of SSDM 2011*, 1300 (2011).
- [3] X. Wu, *et al.*, PRL **101**, 026801 (2008).
- [4] D. Elias, *et al.*, Science **323**, 610 (2009).
- [5] B. Li, *et al.*, ACS Nano **5**, 5957 (2011).
- [6] R. Nair, *et al.*, Small **6**, 2877 (2010).
- [7] F. Banhart, *et al.*, ACS Nano **5**, 26 (2011).
- [8] D. Appelhans *et al.*, New J. Phys. **12**, 125006 (2010).
- [9] D. Boukhvalov and M. Katsnelson, Nano Lett. **8**, 4373 (2008).
- [10] X. Peng and R. Ahuja, Nano Lett. **8**, 4464 (2008).
- [11] A. Stone and D. Wales, Chem. Phys. Lett. **128**, 501 (1986).
- [12] L. Tapaszto, *et al.*, PRB **78**, 233407 (2008).
- [13] G. Liu, *et al.*, IEEE Trans. Nano **10**, 865 (2011).
- [14] H. Hiura, *et al.*, APEX **3**, 095101 (2010).
- [15] M. Lemme, *et al.*, ACS Nano **3**, 2674 (2009).
- [16] D. Bell, *et al.*, Nanotechnology **20**, 455301 (2009).
- [17] M. Han, *et al.*, PRL **104**, 056801 (2010).